Review

Lili Du, Wenjuan Xiong, Wai Kin Chan and David Lee Phillips*

Photoinduced electron transfer processes of single-wall carbon nanotube (SWCNT)–based hybrids

https://doi.org/10.1515/nanoph-2020-0389
Received July 10, 2020; accepted September 22, 2020;
published online October 7, 2020

Abstract: In this review, noncovalent functionalization of single-wall carbon nanotubes (SWCNTs) is briefly reviewed. The functional materials summarized here include metalloporphyrin derivatives, biomolecules and conjugated polymers. Notably, time-resolved spectroscopic techniques such as time-resolved fluorescence and transient absorption were employed to directly investigate the electron transfer and recombination processes between the functionalities and the SWCNTs. In addition, Raman spectroscopy is also useful to identify the interaction and the electron transfer direction between both the functionalities and the SWCNTs. An improved understanding of the mechanisms of these SWCNT-based nanohybrids in terms of their structural and photophysical properties can provide more insights into the design of new electronic materials.

Keywords: electron transfer; light harvesting; photosensitizer; SWCNT; time-resolved spectroscopy.

1 Introduction

Single-wall carbon nanotubes (SWCNTs) with small band gaps, high charge mobilities and current capacities have been widely explored in electronic devices [1, 2]. The strong binding energy between SWCNTs makes it hard to achieve individually dispersed SWCNTs [3]. Both covalent and noncovalent functionalizations were well developed to make well dispersed stable SWCNT solutions. In this review, only the noncovalent methods of functionalizing the sidewalls of SWCNTs will be discussed for the importance of preserving the sp^2 nanotube structure and the electronic properties accordingly.

Photoactive molecules such as light-harvesting molecules which functionalized carbon nanotubes (CNTs) have been shown to be useful materials for photocatalytic and light energy conversion applications [4, 5]. Electron transfer is a crucial step in the conversion of solar energy to photochemical and photoelectrical energy in solar cells or artificial photosynthesis. Functionalization of CNTs with light harvesting molecules to form hybrid nanomaterials can be incorporated into optoelectronic devices. Generally, when the CNT conduction and valence band extrema are sandwiched between the highest occupied molecular orbital (HOMO) and Lowest unoccupied molecular orbital (LUMO) of the photosensitizer molecules [6, 7], energy transfer from the sensitizer to SWNCTs would be predominant [8]. If the photosensitizer and CNT formed a type-II heterojunction, efficient exciton dissociation could be obtained. Electron transfer from the LUMO of the photosensitizer to the conduction band of CNTs and hole transfer from the half-filled HOMO of the photosensitizer to the valence band of CNTs could be achieved [9, 10]. When CNTs are excited directly, the excitons generated will rapidly relax to the ground state before transferring an electron to the photosensitizing molecules due to its very short lifetime [11]. Therefore, the photophysics and electron transfer processes in photosensitizing molecules/CNT hybrids with photoexcitation of the photosensitizing molecules are widely studied. In addition, on introduction of electron donating or withdrawing moieties onto the surface of SWCNTs, extra charge carriers may be generated on the SWCNT surface upon photoexcitation which are exploitable for electronic applications.

In this review, the strategies for noncovalently functionalize the SWCNTs in the last decade, from using small

Lili Du and Wenjuan Xiong contributed equally to this work.

***Corresponding author: David Lee Phillips**, Department of Chemistry, The University of Hong Kong, Hong Kong S.A.R., P.R. China, E-mail: phillips@hku.hk. https://orcid.org/0000-0002-8606-8780
Lili Du, School of Life Sciences, Jiangsu University, Zhenjiang 212013, P.R. China; and Department of Chemistry, The University of Hong Kong, Hong Kong S.A.R., P.R. China
Wenjuan Xiong and Wai Kin Chan, Department of Chemistry, The University of Hong Kong, Hong Kong S.A.R., P.R. China

molecules up to employing supramolecular architectures are reviewed. The Raman spectroscopy and time-resolved spectroscopy results of those functionalities/SWCNT constructs are presented in this review. The mechanism studies including the dynamics of the photoinduced electron transfer and the recombination process in the donor–acceptor systems of interest are mainly highlighted in this work.

2 Metalloporphyrin/SWCNT hybrids

Due to the light harvesting properties of metal complexes, they have been popular in serving as the electron donor in many photosensitizer/SWCNT hybrids. One of the most widely studied photoactive metal complexes has been metalloporphyrin [12]. Even though the metal-free porphyrin was able to disperse and functionalize a number of SWCNTs by noncovalent π–π interaction [13, 14], only the energy transfer process with less than 100 fs was observed from porphyrin to SWCNTs by a transient absorption spectroscopy study [15], which indicates that the direct interaction between the photosensitizer and the SWCNTs might not be a useful idea. Therefore, lots of groups preferred to develop photosensitizer/linker/SWCNT systems to limit the short-range excited state energy transfer process and generate the charge separated states within the hybrids instead. Notably, pyrene was used as the linkage in some systems due to the strong π–π interaction between the pyrene and SWCNT [16].

A series of self-assembly zinc porphyrin derivatives noncovalently linked to SWCNT hybrids have been designed by D'Souza and Ito et al. [8, 17–22], among which the self-assembly mechanisms like the metal–ligand axial coordination, ion pairing, hydrogen bonding and dipole ion pairing have all been reported. As shown in Figure 1a, the self-assembly $(TMPyP^{+})$Zn/$PyrCOO^{-}$/SWCNT and $(TPPS^{-})$Zn/$PyrNH_3^{+}$/SWCNT hybrids were designed through ion paring [17]. According to the energy level diagrams in Figure 1b, the reversible charge seperation (CS) processes were postulated: the CS-1 process refers to the electron transfer process from the LUMO of $(TPPS^{-})$Zn complex to the conduction band of the SWCNT while the CS-2 process refers to the electron transfer process from the valence band of the SWCNT to the HOMO of the $(TMPyP^{+})$Zn complex. This postulation was confirmed by results from picosecond time-resolved fluorescence (ps-TRF) and nanosecond transient absorption (ns-TA) experiments. For the $(TPPS^{-})$Zn/$PyrNH_3^{+}$/SWCNT hybrid, efficient fluorescence quenching was observed after excitation with lifetimes of 290 ps for SWCNT(6, 5) and 140 ps for SWCNT(7, 6), which indicate that a larger diameter SWCNT shows a higher efficiency due to the wider π–π interaction. Thus, we will focus on the discussion of the SWCNT(7, 6) below. In addition, both the radical ions $[(TPPS^{-})Zn]^{\bullet+}$ and $[SWCNT]^{\bullet-}$ were observed by employing ns-TA. In Figure 1c, the transient absorption band at 680 nm was assigned to the ZnP radical cation ($[(TPPS^{-})Zn]^{\bullet+}$) and the broad absorption band at 1400 nm was attributed to the radical cation $[SWCNT]^{\bullet-}$, which decay in about 500–1000 ns. Furthermore, electron-pooling measurements were performed to prove the existence of $[(TPPS^{-})Zn]^{\bullet+}$ and $[SWCNT]^{\bullet-}$ transient species by the addition of the second electron acceptor hexyl viologen dication (HV^{2+}) and a sacrificial electron donor 1-benzyl-1,4-dihydronicotinamide (BNAH) into the hybrid solution. Upon irradiation by 532-nm laser light, the ZnP moiety in the nanohybrids was selectively excited, while the accumulation of $HV^{\bullet+}$ absorption was observed, and the concentration of the accumulated $HV^{\bullet+}$ increased with the BNAH concentration. This is due to that the HV^{2+} extracted the electron trapped in the SWCNT, generating $HV^{\bullet+}$. Meanwhile, the BNAH neutralizes irreversibly $[(TPPS^{-})Zn]^{\bullet+}$ in the nanohybrids, giving $BNAH^{\bullet+}$, finally converted to BNA^{+} (Figure 1d). Similar self-assembly systems [8, 12, 16, 18–23] by employing metal–ligand coordination, cation dipole and hydrogen boding were also demonstrated to be successful photosensitizer–SWCNT-based donor–accepter hybrids, which indicate there is great potential for ZnP/pyrene/SWCNT nanohybrids in light energy harvesting and photovoltaic applications.

3 Biomolecule/SWCNT hybrids

With the development of DNA nanotechnology, the DNA–SWCNT bionanohybrids have shown high impact in lots of areas, such as for biosensors [24], DNA sequencing [25] and structure recognition [26]. D'Souza et al. [27] have also reported the electron transfer process of the porphyrin, ssDNA and SWCNT bionanohybrids ($(TMPyP^{+})$M/ssDNA/SWCNT), M refers to Zn or H_2. As shown in Figure 2a, the ssDNA that acted as the electron mediator between the $(TMPyP^{+})$M and SWCNTs was used to wrap around the sidewalls of SWCNTs helically and attract the $(TMPyP^{+})$M by ion pairing bonding. Comparing with the $(TMPyP^{+})H_2$, $(TMPyP^{+})$Zn system was not only a better electron donor but also had a higher charge stabilization ability; therefore, we will focus on the discussion of $(TMPyP^{+})$Zn below. As displayed in Figure 2b, a similar

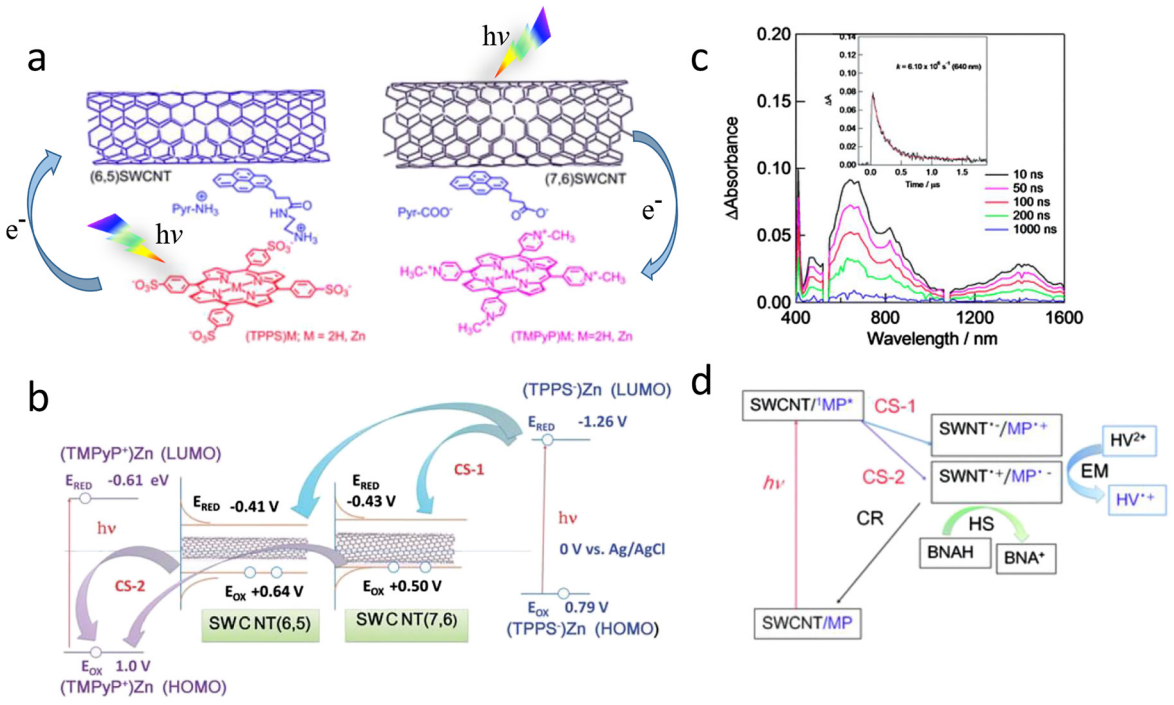

Figure 1: (a) Schematic diagram of photoinduced electron transfer of the $(TPPS^{-})Zn/PyrNH^{3+}$/SWCNT(7, 6) hybrid, (b) Energy level diagram of MP (M = Zn and H_2)/Pyr/SWCNT(*n*, *m*) in polar media, (c) ns-TA of $(TPPS^{-})Zn/PyrNH^{3+}$/SWCNT(7, 6) observed by 532-nm laser irradiation in Ar-saturated Dimethylformamide (DMF). Inset: absorption–time profile at 640 nm, and red curve is the first-order fitting of this data, (d) Mechanism for the electron-pooling process [17]. ns-TA, nanosecond transient absorption; SWCNT, single-wall carbon nanotube.

schematic diagram as Figure 1b was obtained, except for the addition of the LUMO and HOMO energy for ssDNA, which makes the electron transfer from the valence band of the SWCNT to the half-vacant HOMO of ssDNA possible and leads to the formation of the $(TMPyP^{+})Zn^{\bullet-}$ and $SWCNT^{\bullet+}$ ion pair immediately. Therefore, with the help of ssDNA, the invertible CS processes between the $(TMPyP^{+})Zn$ and SWCNTs are proposed as CS-1 and CS-2, respectively, in Figure 2b, although the latter one lacks of strong evidence. As a results, the fluorescence quenching study (Figure 2c) indicated that the quenching of $^{1}(TMPyP^{+})Zn^{*}$ by ssDNA/SWCNT was mainly due to electron transfer instead of energy transfer. The electron transfer rates $k_{CS\text{-}1}$ were 3.9×10^{9} and 5.0×10^{9} s^{-1} for $(TMPyP^{+})Zn$/ssDNA/SWCNT(6, 5) and $(TMPyP^{+})Zn$/ssDNA/SWCNT(7, 6), respectively, as obtained by ps-TRF in Figure 2d. Further evidence for the charge transfer process was provided by the direct observation of radical ions through ns-TA results as shown in Figure 2e and f. As discussed above, the transient band at 660 nm was due to the absorption of $(TMPyP^{+})Zn^{\bullet+}$, and the band at 1250–1300 nm was assigned to the $SWCNT^{\bullet-}$. Comparing with SWCNT(7, 6) $^{\bullet-}$ in Figure 2e, the transient absorption bands for SWCNT(6, 5) $^{\bullet-}$ are more smooth and less intense but show an additional band around 1000 nm which is identical. The charge recombination (CR) rates k_{CR} for the two bionanohybrids $(TMPyP^{+})Zn$/ssDNA/SWCNT(6, 5) and $(TMPyP^{+})Zn$/ssDNA/SWCNT(7, 6) are 6.4×10^{9} and 8.1×10^{9} s^{-1}, respectively. Thus, the ratio k_{CS}/k_{CR} for SWCNT(6, 5) and SWCNT(7, 6) is 540 and 470, respectively, which indicates there is a slightly better charge stabilization ability for SWCNT(6, 5) than SWCNT(7, 6).

Other than DNA, peptides [28] and proteins [16, 29–31] have also been employed to functionalize the sidewalls of SWCNTs by π–π stacking with the development of protein design. López-Andarias et al. [31] designed a consensus tetratricopeptide repeat protein (CTRP) with covalent contacts of porphyrin derivatives and created protein/SWCNT bionanohybrids. As show in Figure 3a, both the Tyr and His residues in each repeat fragment of a CTRP were demonstrated to have strong π–π interaction with the sidewall of SWCNTs while the CTRP8 (repeat number 8) and SWCNT(7, 6) exhibited great compatibility between the concave face of the protein and the surface of SWCNTs. The zinc porphyrin (P) was conjugated with different sizes of proteins by using maleimide–cysteine chemistry as consensus tetratricopeptide repeat protein- Zinc porphyrin (CTPR–P) in different repeat numbers. As shown in Figure 3b, the absorption band at 430 nm was referred to the Soret band of P and was not affected by the

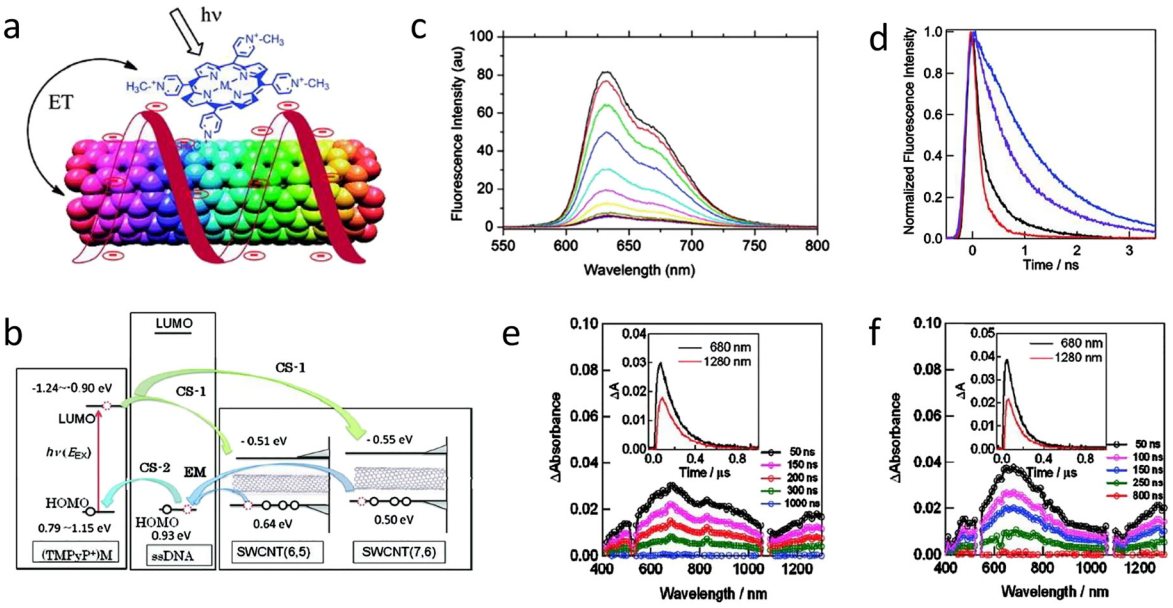

Figure 2: (a) Schematic description of the (TMPyP⁺)M/ssDNA/SWCNT bionanohybrids, (M = Zn or H_2), (b) scheme of the energy-level diagram for the photoinduced electron transfer processes, (c) steady-state fluorescence spectral changes of (TMPyP⁺)Zn (10 μM) on addition of ssDNA/SWCNT(7, 6) in H_2O (λ_{ex} = 435 nm), (d) fluorescence decays of (TMPyP⁺)Zn in H_2O (λ_{ex} = 408 nm). Lines from right to left are (TMPyP⁺)Zn, addition of ssDNA, addition of ssDNA/SWCNT(6, 5) and addition of ssDNA/SWCNT(7, 6), (e, f) ns-TA of (TMPyP+)Zn/ssDNA/SWCNT(*n*, *m*) observed by 532 nm laser light irradiation in H_2O, (e) SWCNT(6, 5) and (f) SWCNT(7, 6) [27]. ns-TA, nanosecond transient absorption; SWCNT, single-wall carbon nanotube.

size of the proteins, which indicated the effectiveness of the qualitative conjugation reaction between P and the CTPRs. Raman spectroscopy was employed to study the interactions between the electron donor–acceptor bionanohybrids in Figure 3c and d. The intensity for both the D band and the G band of the CTPR16/SWCNT and CTPR16-P/SWCNT remains the same when compared to the pristine SWCNT as shown in Figure 3c, which reveals there is mainly noncovalent interaction between the proteins and the SWCNTs. In Figure 3d, the G band of both hybrids showed downshifts to 1589 cm^{-1} for CTPR16/SWCNT and to 1585 cm^{-1} for CTPR16-P/SWCNT. In analogy with the original G band at 1592 cm^{-1} for the pristine SWCNT, it indicates that the SWCNT acted as an electron acceptor in the hybrid systems. Obviously, an enhanced effect (7 cm^{-1}) was observed for the CTPR16-P/SWCNT, and it makes the electron transfer from the zinc phorphyrins to the SWCNTs possible. In addition, the flash photolysis microwave conductivity technique was also used to study the injection and transportation processes of the photoinduced charge carriers between the protein/SWCNT systems. With the presence of SWCNTs, all the hybrids maintain the conductivity property and generate mobile charge carriers after excitation at 355 and 420 nm. The second-order recombination kinetics elucidates that the diffusion of the electrons on the SWCNT determines the recombination process of the electrons and holes. Even though the time-resolved spectroscopy study of this work was not sufficient, the first dynamics study of the protein/SWCNT hybrids implied there may be potential applications of these systems in biomolecular electronics.

4 Polymer/SWCNT hybrids

Conjugated polymer wrapping has been developed as one of the most promising methods to disperse and purify SWCNTs [32]. Polymers like regioregular poly(3-alkylthiophene)s (P3AT) [33], poly(9,9-dialkylfluorene)s [34–36], poly(phenylene vinylene) (PPV) [37] and poly(phenylene ethynylenes) [38] were demonstrated to be efficient SWCNT dispersants, some of which presented excellent SWCNT diameter and chirality selectivity [32]. Functional molecules/groups covalently linked to the polymer side chain which act as the pending arms along the polymer main chain have been reported [39–41]. Meanwhile, strong electron acceptros or metal complexes immobilized into the polymer main chain and directly placed on the surface of SWCNT is another method to endow the polymer/SWCNT hybrids unique properties [42–44]. Conjugated polyelectrolyte can be used to selectively dope SWCNTs by varying the ionic functionalities [45].

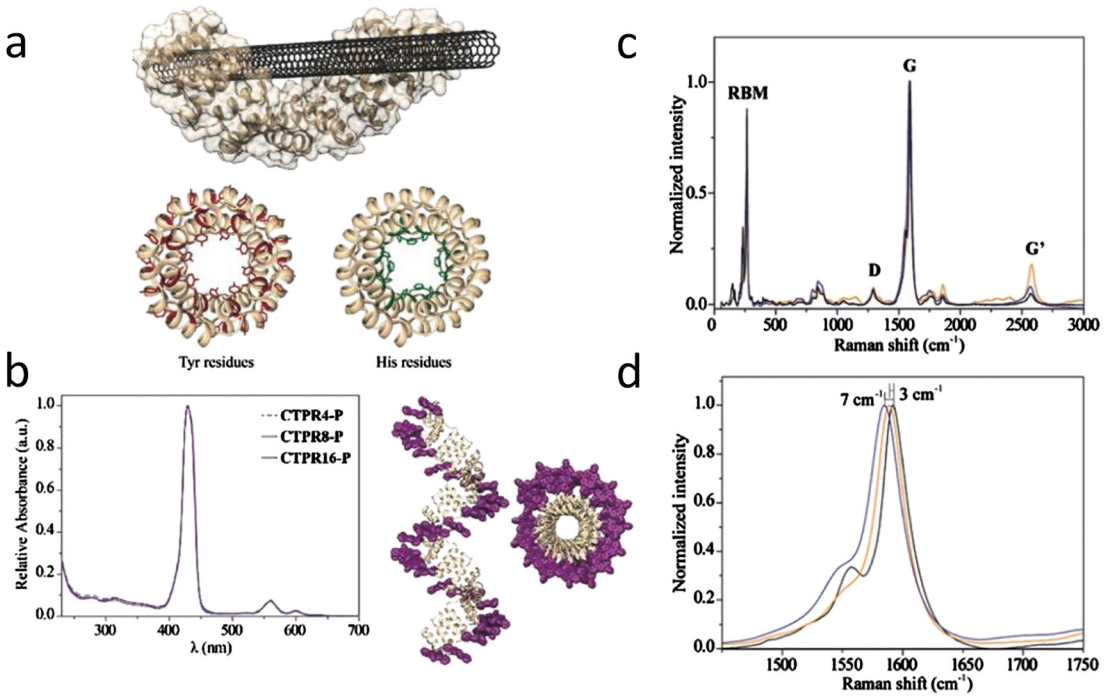

Figure 3: (a) Model morphology of the CTPR8/SWCNT(7, 6) hybrid with an axial view of the Tyr residues (red) and the His residues (green), (b) normalized UV–vis spectra of the conjugates CTPR4-P, CTPR8-P and CTPR16-P with presentation of CTPR16-P from different views, (c) Raman spectra of pristine SWCNTs (black), CTPR16/SWCNT (yellow), CTPR16-P/SWCNT (purple) after excitation at 785 nm, (d) normalized Raman spectra in the region of the G-mode [31]. SWCNT, single-wall carbon nanotube.

Time-resolved transient spectroscopies are strong tools to study the interactions between the conjugated polymer and SWCNTs, which provide a systematic and theoretical instruction to develop more efficient systems. In light-sensitive polymer/SWCNT hybrids, the generation and separation of free charges and polarons at the interface between the conjugated polymer and the SWCNT upon photoexcitation is crucial for the efficiency of organic photovoltaic (OPV) solar cells [46, 47]. Through the use of time-resolved transient spectroscopy techniques, the charge separation, mobilization and recombination processes can be monitored and studied. The dynamics of the generated charge carriers is exploitable for electronic applications. P3HT/SWCNT hybrids are widely used in electronic devices [47–49]. In the hybrids, SWCNTs acted as efficient acceptors while P3HT acted as donors due to their work function alignment. Both P3HT and SWCNT possess excellent hole and charge mobility. However, devices based on SWCNT blends with conjugated polymers have generally shown poor performance to date [50, 51]. In large diameter P3HT/SWCNT hybrids, the energy transfer from the P3HT to SWCNT was predominant and efficient, so this results in the limitation of the charge separation, which might be the reason for the poor performance of the device [52].

As for small diameter SWCNTs, individually dispersed SWCNTs wrapped by a single molecular layer of P3HT were reported as shown in Figure 4a [53]. An ultrafast charge transfer process from the P3HT to SWCNT across the interface was observed by time-correlated single photon counting (TCSPC), photoluminescence upconversion (PLUC) and femtosecond transient absorption (fs-TA). According to a PLUC and TCSPC study in Figure 4b, P3HT decays with two time constants of 1.7 and 689 ps. However, the emission of P3HT in the P3HT/SWCNT film decays with an ultrafast time constant of 0.43 ps (Figure 4b red squares), which indicates there is a fast exciton quenching process with the presence of SWCNTs comparing to pure bulk P3HT. Besides, fs-TA was also utilized to confirm the presence of a charge separation process as proposed in the PLUC study in Figure 4c. For comparison, the conventional 6:4 blend of P3HT and [6,6]-phenyl-C_{61}-butyric acid methyl ester (PCBM) (P3HT-PCBM) was also investigated for their great photon-to-charge conversion ratios. The stimulated emission observed for bulk P3HT decays rapidly and this is mainly due to the exciton–exciton annihilation without generation of the long-lived charge-separated species (blue circles). Unlike the bulk P3HT, the P3HT/SWCNT hybrids exhibit significant differences in their fs-TA (black diamonds): instead of observation of the negative stimulated

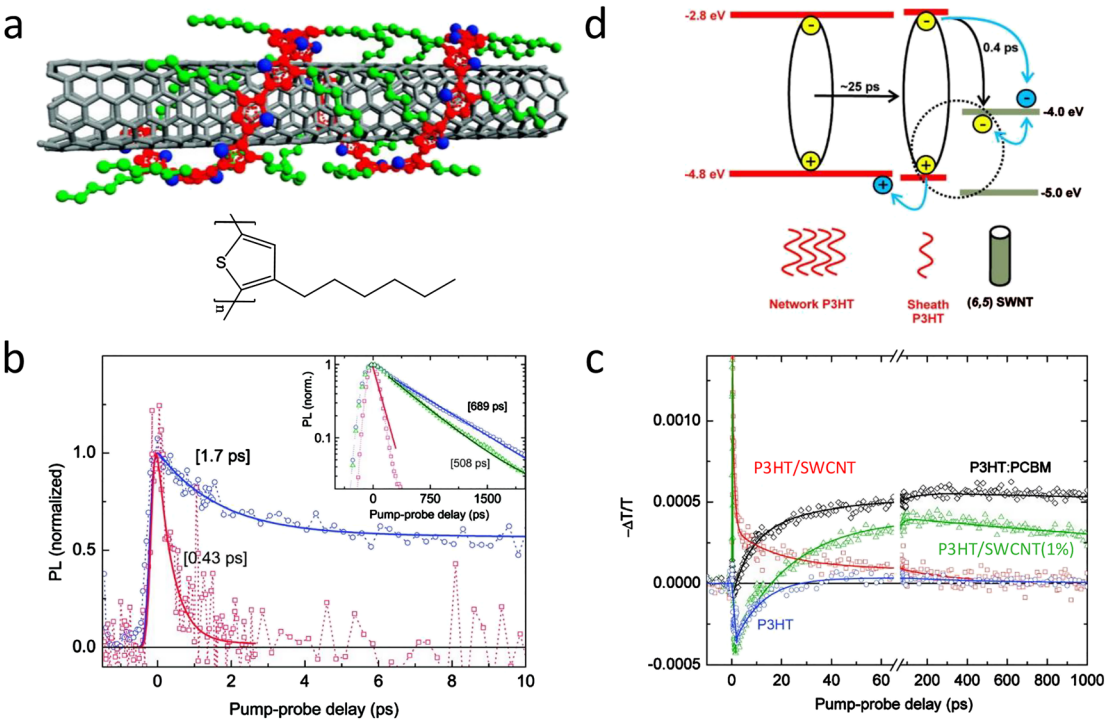

Figure 4: (a) Chemical structure of P3HT and schematic diagram of a SWCNT(6, 5) coated with a monolayer of sheath P3HT; (b) The emission of the P3HT (blue circles) was detected at 660 nm and P3HT/SWCNT (red squares) was detected at 620 nm after 400 nm excitation. Inset: TCSPC decay curves at the same probe wavelengths used for PLUC. The P3HT/SWCNT(1%) (green triangles) sample was also detected at 660 nm; (c) Kinetics obtained through fs-TA for the P3HT-PCBM (black diamonds), P3HT (blue circles), P3HT/SWNT (red squares) and P3HT/SWNT(1%) (green triangles) after irradiation by 400 nm and probed at 730 nm; (d) Scheme to illustrate the observed charge generation dynamics for a P3HT sheath monolayer around a SWCNT(6, 5) with an excess of P3HT acting as a surrounding network [53]. SWCNT, single-wall carbon nanotube; TCSPC, time-correlated single photon counting; PLUC, photoluminescence upconversion; fs-TA, femtosecond transient absorption.

emission, an absorption band increased within 350 fs, and this feature is assigned to free polarons generated from charge dissociation of the P3HT excitons at the heterointerface of P3HT/SWCNT hybrids, which is consistent with the PLUC study. The holes on the P3HT decay through charge recombination process around 10–100 ps due to the confined structures. However, the extra P3HT in P3HT/SWCNT(1%) hybrids can inhibit the charge recombination process. As shown in Figure 4c (green triangles), stimulated emission arising within 10 ps implicates the generation of a large amount of excitons in the network of P3HT when excess P3HT exists in the P3HT/SWCNT(1%) hybrids. Then, the free polarons are generated due to fast dissociation of the excitons in the interface between P3HT and SWCNT in 25 ps as displayed in Figure 4d. With the help of extra P3HT, the hole can migrate away from the interface, and this leads to long-lived charge separated states. A similar dynamics between the P3HT-NT (1%) (green) and the P3HT-PCBM (60:40) (black) in Figure 4c indicates that the P3HT-NT (1%) sample produces a similar efficiency of charge separation to that observed in an optimized 60:40 blend of P3HT-fullerene. These findings thus establish a promising route for developing efficient OPV devices utilizing polymer–SWCNT blends.

Since P3AT has excellent dispersion properties, as well as electronic and light absorption properties, it was utilized as a dispersant and intermediate to link functional moieties into the hybrids [40, 41]. Our group published a hybrid system in which the SWCNT was wrapped and dispersed by regioregular poly(thiophene) functionalized with a pendant photosensitizing ruthenium complex (Figure 5a) [41]. Incorporation of the photosensitizers into the polymer systems could produce a polymeric array with a combination of beneficial properties such as having a high optical cross section and higher dispersing power for the SWCNT. The dynamics of the photoinduced electron transfer process between the ruthenium sensitizers and SWCNTs was probed by fs-TA. For polymer 5, upon excitation, both the Ru complex and the polythiophene were excited. As shown in Figure 5b, the Ru complex ^{1}MLCT excited states undergo a rapid intersystem crossing (ISC) process to the ^{3}MLCT excited states within the instrument

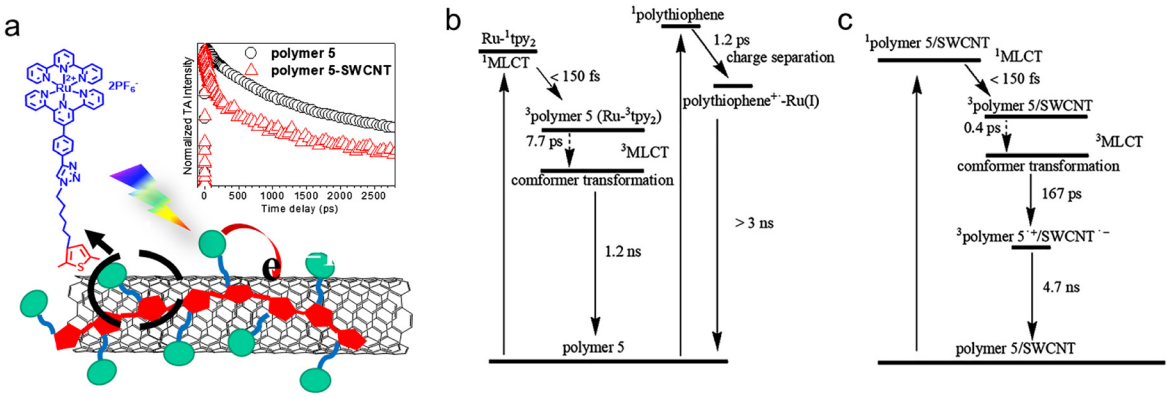

Figure 5: (a) Schematic illustration of the polymer 5/SWCNT hybrid, the decay kinetics at 680 nm achieved by fs-TA of both polymer 5 and the polymer 5/SWCNT hybrids is shown as inset diagrams; (b) Schematic diagram showing the photophysical processes in polymer 5; (c) The charge injection process in the polymer 5/SWCNT hybrid (right) [41]. fs-TA, femtosecond transient absorption; SWCNT, single-wall carbon nanotube.

response time (<150 fs). Meanwhile, an electron transfers from the polythiophene singlet excited state to Ru(II) within 1.2 ps to form a charge separated state. The Ru complex undergoes a torsional relaxation of the excited state species to a more planar structure in 7.7 ps. After that, the polythiophene$^{\bullet+}$-Ru(I) decays over 3 ns, and the ^{3}MLCT of Ru complex species decays in about 1.2 ns.

After the formation of the polymer 5/SWCNT hybrid, upon excitation, the polymer undergoes a rapid intersystem crossing to generate the ^{3}polymer 5/SWCNT within the instrument response time (<150 fs) in Figure 5c. Then, the polymer undergoes the torsional relaxation of the polymer 5 ^{3*}MLCT excited state in ~0.4 ps in a similar manner as polymer 5. After that, the polymer 5 ^{3}MLCT excited state decays with the formation of the charge-separated state polymer 5$^{\bullet+}$/SWCNT$^{\bullet-}$ in ~167 ps. The charge recombination process takes a longer time around 4.7 ns. A fast electron transfer process from the sensitizing Ru(II) complex to SWCNTs with a time constant of 167 ps was revealed by ultrafast transient absorption spectroscopy. The system presented here may serve as a model for the design of new light harvesting systems based on polymer/SWCNT hybrids.

Poly(9,9-didodecylfluorene-2,7-diyl- and poly (3-dodecylthiophene)-dispersed SWCNTs were studied by Fourier transform infrared spectroscopy, which is a useful method to observe the polymer's polaron absorption [54]. These results implicated that polymer-wrapped CNTs should be considered as a single hybrid system, exhibiting states shared between the two components, since no matter the excitation wavelength is above or below the polymer band gap, polarons are generated in the polymers.

Pendent zinc phthalocyanines (ZnPcs) covalently linked to the backbone of poly(*p*-phenylene vinylene) (PPV) oligomers via an ether linker have been explored to disperse SWCNTs [55, 56]. When PPV was substituted by electron-withdrawing –CN groups, the *p*-type PPV changed to *n*-type. Due to the strong electron withdrawing ability of the –CN group, the repelling force between the relatively *p*-type SWCNT and *p*-type PPV was reduced and a strengthened π–π interaction was achieved. A homogeneous and stable dispersed SWCNT suspension was achieved. ZnPcs are electronically "isolated" from the PPV by an ether linkage; therefore, the *n*-type character of the CN–PPV is not affected by the presence of the ZnPc units. After irradiation, a metastable radical ion pair state composed of oxidized ZnPc and reduced SWCNT oxidized was generated. Remarkably, the ratio of charge separation to charge recombination is nearly three orders of magnitude compared to hybrid without –CN.

In addition to –CN, many other electron-withdrawing groups like perylene [57–59] derivatives have been introduced into the polymer main chain and directly immobilized onto the SWCNT surface to form well-dispersed suspensions [44]. A perylenediimide (PDI) acceptor containing chiral polymer (S-PBN(b)-Ph$_4$PDI) dispersed (6, 5) chirality-enriched SWCNTs ([SWCNTs (6, 5)] was reported [44]. The PDI electron acceptor unit was found to be positioned at 3 nm intervals on the surface of the SWCNT, which means that the SWCNT/electron acceptor stoichiometry and organization can be rigorously controlled. The charge separation (CS) and CR processes were studied by the transient absorption spectroscopy. Upon excitation with a 1000-nm laser pulse, a new band centered at 1120 nm was observed and it rapidly decayed over 5 ps (Figure 6a). Another new absorption feature at 1155 nm emerges at ~0.5 ps and becomes clear after 2 ps. The transient absorption band centered at 1155 nm is related to the SWCNT hole polaron state SWCNT$^{(\bullet+)n}$. The SWCNT$^{(\bullet+)n}$ transient state nature was confirmed by adding the chemical oxidant (0.5 mm K_2IrCl_6

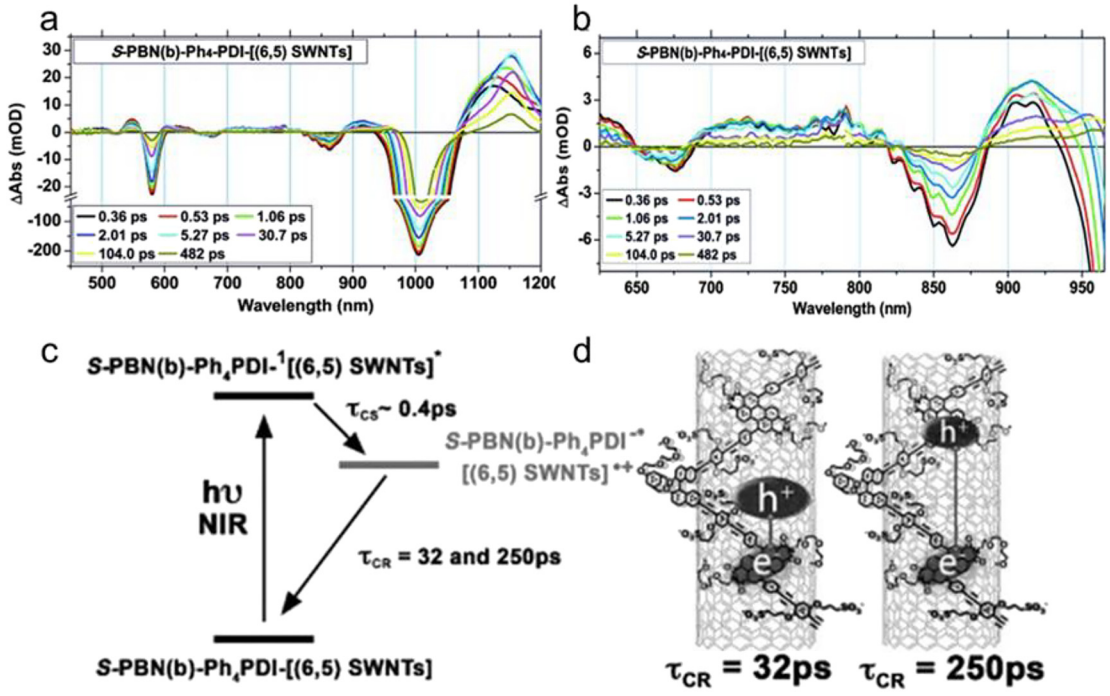

Figure 6: (a) and (b) Representative transient absorption spectra recorded for S-PBN(b)-Ph_4PDI-[SWNT(6, 5)] samples dispersed in 3:7 MeOH/D_2O at the time delays noted. λ_{ex} = 1000 nm; (c) Representation of the photoinduced charge separation (CS) and thermal charge recombination (CR) dynamics observed following $E_{00} \rightarrow E_{11}$ excitation (λ_{ex} = 1000 nm) for the S-PBN(b)-Ph_4PDI-[SWCNT(6, 5)] nanoscale assembly; (d) CR dynamics involving both an intimately associated SWCNT hole polaron and $PDI^{\bullet-}$ and a related charge-separated state involving $PDI^{\bullet-}$ and a SWCNT hole polaron derived from charge migration to an adjacent hole polaron site along the SWCNT backbone [44]. SWCNT, single-wall carbon nanotube.

[+0.65 V vs. SCE in H_2O]) to the SWCNT solution and traced by steady-state electronic absorption spectroscopy [60, 61]. More recent studies have shown that, this ~1150 nm band is related to exciton polaron species, i.e., excitons dressed in the Fermi sea of charge carriers; and due to this reason, both the so-called "electron polaron" and "hole polaron" share the same spectroscopic signatures at ~1150 nm [62–64]. Transient absorption bands centered at 625–800 nm and 880–950 nm are assigned to the polymer radical anion (Figure 6b). The formation of the polymer radical anion was confirmed by the reductive reaction using a reductive titration of the S-PBN(b)-Ph_4PDI polymer with sodium dithionate (–0.90 V vs. SCE) in 3:7 MeOH/D_2O. New absorption bands centered at 755, 844, 902 and 1032 nm were formed during the reductive titration experiments, which correspond to the $PDI^{\bullet-}$ radical anion. Multiwavelength global analysis was utilized to extract the time constants for the photoinduced charge separation (τ_{CS}) and thermal charge recombination (τ_{CR}). Monitoring the rise of the PDI (523.7 nm) and SWCNT (578.5 and 1004.9 nm) ground-state bleach signals and the rise of the transient absorptive signature of the ET products $SWCNT^{(\bullet+)n}$ (1154.9 nm) and $PDI^{\bullet-}$ (701.0, 753.9, 849.9 and 904.5 nm) determines $\tau_{CS} \approx 0.4$ ps (φ_{CS} = 97%). The decay dynamics of the $SWCNT^{(\bullet+)n}$ and $PDI^{\bullet-}$ transient absorptive signatures provide two charge recombination time constants ($\tau_{CS} \approx 31.8$ and 250 ps) (Figure 6c). The two charge recombination rates may due to the charge recombination of the $PDI^{\bullet-}$ and an intimately close SWCNT hole polaron (31.8 ps), and a recombination of the $PDI^{\bullet-}$ and a hole polaron migrated along the SWCNT from other polaron sites (250 ps) (Figure 6d). This work thus defines a viable strategy to control the stoichiometry of electron (hole) acceptors at the nanotube interface, regulate the hole (electron) polaron density generated per nanotube unit length for a defined set of irradiation conditions and also enable to engineer nanotube–soft matter assemblies in which the critical energy transduction dynamical processes may be modulated.

Our group [65] reported SWCNTs dispersed by conjugated polymers incorporated with cycloplatinated complexes (P1–Pt and P2–Pt) (Figure 7a). Both polymers showed good SWCNT dispersion ability, and stable well-dispersed polymer/SWCNT hybrids solutions were obtained. The photoinduced electron transfer processes in these hybrids were studied by Raman and fs-TA spectroscopy. The G band of P2–Pt/SWCNT upshifts from 1598 to 1602 cm^{-1}, and the G band of P1–Pt/SWCNT downshifts

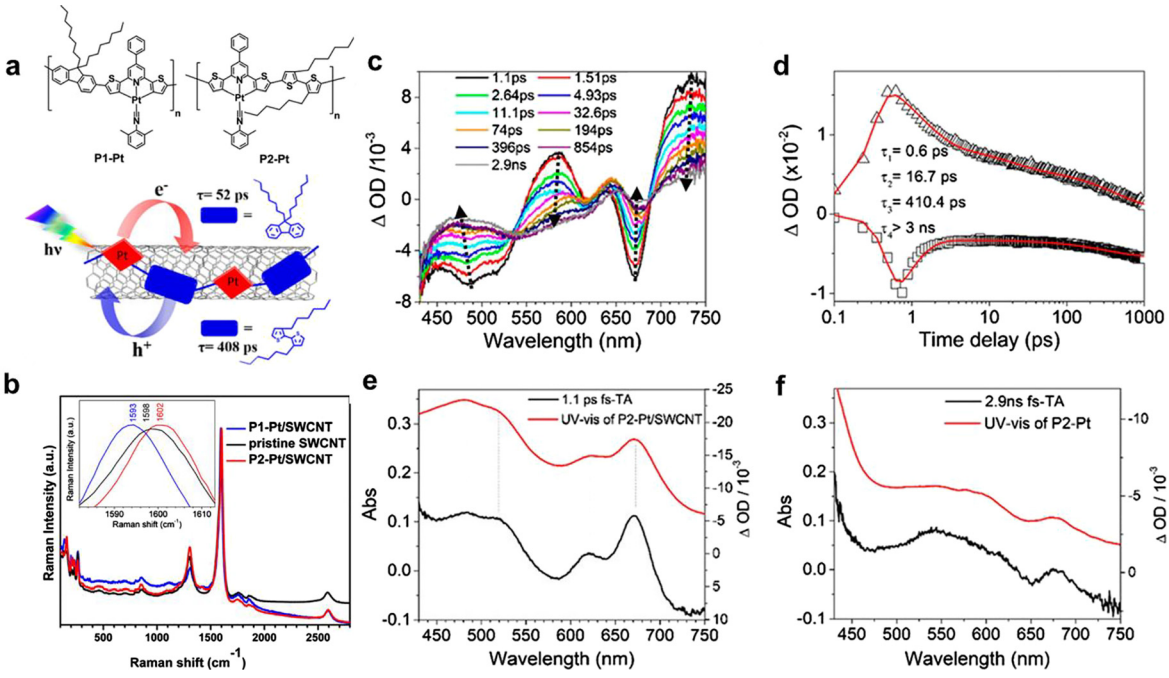

Figure 7: (a) Polymer structures and schematic presentation of polymer/SWCNT hybrids; (b) micro-Raman spectra of pristine SWCNTs (black), P1–Pt/SWCNT (blue) and P2–Pt/SWCNT (red) (excited at 785 nm); (c) fs-TA of P2–Pt/SWCNT in THF solution acquired after 400 nm irradiation; (d) kinetic traces at 730 nm (black triangle), 530 nm (black square) and the respective fitting traces (solid lines, red) based on a global analysis with four exponential functions; (e) comparison between the UV–vis spectra of P2–Pt/SWCNT with the transient absorption spectrum at 1 ps; (f) comparison between the UV–vis spectra of P2–Pt with the transient absorption spectrum at 3 ns [65]. SWCNT, single-wall carbon nanotube; fs-TA, femtosecond transient absorption.

from 1598 to 1593 cm^{-1} after forming hybrids compared to pristine SWCNTs (Figure 7b). It has been reported that the G and RBM bands of SWCNTs would shift to higher frequency upon losing electrons and to lower frequency upon receiving electrons [66]. It is proposed that P1–Pt serves as an electron donor and P2–Pt serves as an electron acceptor upon forming hybrids with SWCNTs. The fs-TA spectra of P1–Pt/SWCNT hybrid are similar to those of the P1–Pt polymer. The kinetics of the decay observed at 490 nm for P1–Pt/SWCNT was fitted by a triexponential function with time constants of 2.7, 52 and 445 ps. The processes occurring at 2.7 and 445 ps are similar to the ISC and solvent relaxation processes observed in P1–Pt. The second time constant at 52 ps is assigned to the electron injection from the triplet excited states of P1–Pt to the SWCNT, resulting in the formation of the charge-separated $P1–Pt^{\bullet+}/SWCNT^{\bullet-}$ species. P2–Pt/SWCNT shows remarkably different photophysical properties compared to the pure P2–Pt polymer (Figure 7c). By comparing the UV–Vis spectra of P2–Pt/SWCNT with the TA spectrum of P2–Pt/SWCNT at 1 ps (Figure 7d), the bleaching bands at 500 and 670 nm are assigned to the ground state bleaching of the SWCNTs, while the positive bands at 590 and 730 nm represent the formation of the SWCNT singlet excited states [67]. Global analysis of the transient decay dynamics reveals four time constants (Figure 7d): 0.6 ps (62%), 16.3 ps (30%), 408 ps (8%) and a fourth one that exceeds the limitation (>3 ns) of the instrument coverage. The processes observed at 0.6 and 16.3 ps were assigned to the exciton–exciton annihilation and singlet exciton recombination [63, 68–70]. However, the long-lived component (408 ps) was not observed previously. As shown in Figure 7c, the bleaching bands show little change at 530 nm after 76 ps, while the intensity of the positive bands drops to zero within the time interval from 76 ps to 3 ns. This could be due to the generation of a new species associated with the decay of the singlet SWCNT excited states. To confirm this, the UV–vis spectra of P2–Pt and the transient absorption spectrum of P2–Pt/SWCNT at 3 ns are compared (Figure 7f). The good agreement between these two spectra strongly suggests an electron transfer process from the SWCNTs to P2–Pt, forming radical anions ($P2–Pt^{\bullet-}$) within 408 ps. The radical anions are long-lived species with a lifetime longer than 3 ns. Therefore, it is concluded that P2–Pt accepts electrons from the SWNCT after forming hybrids with SWCNTs. The results are in good agreement with the micro-Raman spectral data discussed above. The electronic transition energy of the polymer can

be varied by using different cyclometalated and ancillary ligands, and the flow direction of the photoexcited electrons in these hybrids can be tailored and designed by varying the comonomer unit. These polymer–SWCNT hybrids may serve as a model for the design of new SWCNT-based light harvesting systems in which the electron flow direction and the type of carriers can be controlled.

5 Conclusion

The keynote of this review is to describe selected studies on the photoinduced electron transfer process of functionalities/SWCNT hybrids ranging from small systems to larger supramolecular assemblies. The selected functionalities discussed in this paper not only show an excellent ability to disperse the SWCNTs but also combine the intrinsic properties of both functionalities and SWCNTs. For instance, a wider visible light absorption range could be achieved through the high optical cross section of light-harvesting molecules and SWCNTs; DNA or proteins endow SWCNTs to display biocompatible properties, and the hybrids could be utilized for biomedical applications; extra charge carriers could be generated in SWCNTs upon photoexcitation through *n*-type or *p*-type doping. As a conclusion, for variation of the electronic properties of the functionalities, the electron transfer direction in the hybrid systems could be reversibly controlled. Most of the photosensitizers like metalloporphyrin derivatives, biomolecules, electron-rich polymers acted as the electron donors in the hybrids. As such, electron-deficient moieties mobilized onto the surface of SWCNTs accept electrons from the SWCNTs. Time-resolved spectroscopic techniques such as the time-resolved fluorescence and transient absorption were employed to investigate the electron transfer and recombination processes between the functionalities and SWCNTs directly. Even though the assignment for the electron transfer and energy transfer processes is reliable, there are still some ambiguous assignments for some recombination processes, especially involving several reaction pathways that may be seen in complicated supramolecular systems. Therefore, a better understanding for the mechanisms of those SWCNT-based nanohybrids in terms of structural and photophysical properties might provide more insights into the design of new electronic devices.

Acknowledgment: The authors would like to acknowledge the grants from the National Science Fund of China (21803026) and Natural Science Foundation of Jiangsu Province (BK20180854), the Hong Kong Research Grants Council (GRF 17302218, GRF 17302419), The University of Hong Kong Development Fund 2013–2014 project "New Ultrafast Spectroscopy Experiments for Shared Facilities" and Major Program of Guangdong Basic and Applied Research (2019B030302009).

Author contribution: All the authors have accepted responsibility for the entire content of this submitted manuscript and approved submission.

Research funding: The authors would like to acknowledge the grants from the National Science Fund of China (21803026) and Natural Science Foundation of Jiangsu Province BK20180854), the Hong Kong Research Grants Council (GRF 17302218, GRF 17302419), The University of Hong Kong Development Fund 2013–2014 project "New Ultrafast Spectroscopy Experiments for Shared Facilities" and Major Program of Guangdong Basic and Applied Research (2019B030302009).

Conflict of interest statement: The authors declare no competing financial interest.

References

[1] M. F. De Volder, S. H. Tawfick, R. H. Baughman, and A. J. Hart, "Carbon nanotubes: present and future commercial applications," *Science*, vol. 339, no. 6119, pp. 535–539, 2013.

[2] V. Sgobba and D. M. Guldi, "Carbon nanotubes—electronic/electrochemical properties and application for nanoelectronics and photonics," *Chem. Soc. Rev.*, vol. 38, no. 1, pp. 165–184, 2009.

[3] A. Thess, R. Lee, P. Nikolaev, et al., "Crystalline ropes of metallic carbon nanotubes," *Science*, vol. 273, no. 5274, pp. 483–487, 1996.

[4] F. D'Souza and O. Ito, "Supramolecular donor–acceptor hybrids of porphyrins/phthalocyanines with fullerenes/carbon nanotubes: electron transfer, sensing, switching, and catalytic applications," *Chem. Commun.*, no. 33, pp. 4913–4928, 2009. https://doi.org/10.1039/b905753f.

[5] D. M. Guldi, G. M. A. Rahman, F. Zerbetto, and M. Prato, "Carbon nanotubes in electron donor–acceptor nanocomposites," *Acc. Chem. Res.*, vol. 38, no. 11, pp. 871–878, 2005.

[6] G.-J. Wang, M.-W. Lee, and Y.-H. Chen, "A TiO_2/CNT coaxial structure and standing CNT array laminated photocatalyst to enhance the photolysis efficiency of TiO_2," *Photochem. Photobiol.*, vol. 84, no. 6, pp. 1493–1499, 2008.

[7] F. D'Souza and O. Ito, "Photosensitized electron transfer processes of nanocarbons applicable to solar cells," *Chem. Soc. Rev.*, vol. 41, no. 1, pp. 86–96, 2012.

[8] F. D'Souza, A. S. D. Sandanayaka, and O. Ito, "SWNT-based supramolecular nanoarchitectures with photosensitizing donor and acceptor molecules," *J. Phys. Chem. Lett.*, vol. 1, no. 17, pp. 2586–2593, 2010.

[9] T. Schuettfort, A. Nish, and R. J. Nicholas, "Observation of a type II heterojunction in a highly ordered polymer–carbon nanotube

nanohybrid structure," *Nano Lett.*, vol. 9, no. 11, pp. 3871–3876, 2009.
[10] D. O. Bellisario, R. M. Jain, Z. Ulissi, and M. S. Strano, "Deterministic modelling of carbon nanotube near-infrared solar cells," *Energy Environ. Sci.*, vol. 7, no. 11, pp. 3769–3781, 2014.
[11] M. S. Dresselhaus, G. Dresselhaus, R. Saito, and A. Jorio, "Exciton photophysics of carbon nanotubes," *Annu. Rev. Phys. Chem.*, vol. 58, pp. 719–747, 2007.
[12] R. C. Haddon, "Carbon nanotubes," *Acc. Chem. Res.*, vol. 35, no. 12, p. 997, 2002.
[13] J. Chen and C. P. Collier, "Noncovalent functionalization of single-walled carbon nanotubes with water-soluble porphyrins," *J. Phys. Chem. B*, vol. 109, no. 16, pp. 7605–7609, 2005.
[14] A. Satake, Y. Miyajima, and Y. Kobuke, "Porphyrin–carbon nanotube composites formed by noncovalent polymer wrapping," *Chem. Mater.*, vol. 17, no. 4, pp. 716–724, 2005.
[15] D. Garrot, B. Langlois, C. Roquelet, et al., "Time-resolved investigation of excitation energy transfer in carbon nanotube-porphyrin compounds," *J. Phys. Chem. C*, vol. 115, no. 47, pp. 23283–23292, 2011.
[16] R. J. Chen, Y. Zhang, D. Wang, and H. Dai, "Noncovalent sidewall functionalization of single-walled carbon nanotubes for protein immobilization," *J. Am. Chem. Soc.*, vol. 123, no. 16, pp. 3838–3839, 2001.
[17] S. K. Das, N. K. Subbaiyan, F. D'Souza, A. S. D. Sandanayaka, T. Hasobe, and O. Ito, "Photoinduced processes of the supramolecularly functionalized semi-conductive SWCNTs with porphyrinsvia ion-pairing interactions," *Energy Environ. Sci.*, vol. 4, no. 3, pp. 707–716, 2011.
[18] A. S. D. Sandanayaka, R. Chitta, N. K. Subbaiyan, L. D'Souza, O. Ito, and F. D'Souza, "Photoinduced charge separation in ion-paired porphyrin–single-wall carbon nanotube donor–acceptor hybrids," *J. Phys. Chem. C*, vol. 113, no. 30, pp. 13425–13432, 2009.
[19] R. Chitta, A. S. D. Sandanayaka, A. L. Schumacher, et al., "Donor–acceptor nanohybrids of zinc naphthalocyanine or zinc porphyrin noncovalently linked to single-wall carbon nanotubes for photoinduced electron transfer," *J. Phys. Chem. C*, vol. 111, no. 19, pp. 6947–6955, 2007.
[20] S. K. Das, N. K. Subbaiyan, F. D'Souza, A. S. D. Sandanayaka, T. Wakahara, and O. Ito, "Formation and photoinduced properties of zinc porphyrin-SWCNT and zinc phthalocyanine-SWCNT nanohybrids using diameter sorted nanotubes assembled via metal–ligand coordination and π–π stacking," *J. Porphyr. Phthalocyanines*, vol. 15, no. 09n10, pp. 1033–1043, 2011.
[21] E. Maligaspe, A. S. D. Sandanayaka, T. Hasobe, O. Ito, and F. D'Souza, "Sensitive efficiency of photoinduced electron transfer to band gaps of semiconductive single-walled carbon nanotubes with supramolecularly attached zinc porphyrin bearing pyrene glues," *J. Am. Chem. Soc.*, vol. 132, no. 23, pp. 8158–8164, 2010.
[22] F. D'Souza, R. Chitta, A. S. D. Sandanayaka, et al., "Self-Assembled single-walled carbon nanotube: zinc–porphyrin hybrids through ammonium ion–crown ether interaction: construction and electron transfer," *Chem. Eur J.*, vol. 13, no. 29, pp. 8277–8284, 2007.
[23] D. M. Guldi, G. M. A. Rahman, N. Jux, N. Tagmatarchis, and M. Prato, "Integrating single-wall carbon nanotubes into donor–acceptor nanohybrids," *Angew. Chem. Int. Ed.*, vol. 43, no. 41, pp. 5526–5530, 2004.
[24] E. S. Jeng, A. E. Moll, A. C. Roy, J. B. Gastala, and M. S. Strano, "Detection of DNA hybridization using the near-infrared band-gap fluorescence of single-walled carbon nanotubes," *Nano Lett.*, vol. 6, no. 3, pp. 371–375, 2006.
[25] S. Meng, P. Maragakis, C. Papaloukas, and E. Kaxiras, "DNA nucleoside interaction and identification with carbon nanotubes," *Nano Lett.*, vol. 7, no. 1, pp. 45–50, 2007.
[26] X. Tu, S. Manohar, A. Jagota, and M. Zheng, "DNA sequence motifs for structure-specific recognition and separation of carbon nanotubes," *Nature*, vol. 460, no. 7252, pp. 250–253, 2009.
[27] F. D'Souza, S. K. Das, M. E. Zandler, A. S. D. Sandanayaka, and O. Ito, "Bionano donor–acceptor hybrids of porphyrin, ssDNA, and semiconductive single-wall carbon nanotubes for electron transfer via porphyrin excitation," *J. Am. Chem. Soc.*, vol. 133, no. 49, pp. 19922–19930, 2011.
[28] V. Z. Poenitzsch, D. C. Winters, H. Xie, G. R. Dieckmann, A. B. Dalton, and I. H. Musselman, "Effect of electron-donating and electron-withdrawing groups on peptide/single-walled carbon nanotube interactions," *J. Am. Chem. Soc.*, vol. 129, no. 47, pp. 14724–14732, 2007.
[29] T. J. McDonald, D. Svedruzic, Y.-H. Kim, et al., "Wiring-up hydrogenase with single-walled carbon nanotubes," *Nano Lett.*, vol. 7, no. 11, pp. 3528–3534, 2007.
[30] K. Matsuura, T. Saito, T. Okazaki, S. Ohshima, M. Yumura, and S. Iijima, "Selectivity of water-soluble proteins in single-walled carbon nanotube dispersions," *Chem. Phys. Lett.*, vol. 429, no. 4, pp. 497–502, 2006.
[31] J. López-Andarias, S. H. Mejías, T. Sakurai, et al., "Toward bioelectronic nanomaterials: photoconductivity in protein–porphyrin hybrids wrapped around SWCNT," *Adv. Funct. Mater.*, vol. 28, no. 24, p. 1704031, 2018.
[32] S. K. Samanta, M. Fritsch, U. Scherf, W. Gomulya, S. Z. Bisri, and M. A. Loi, "Conjugated polymer-assisted dispersion of single-wall carbon nanotubes: the power of polymer wrapping," *Acc. Chem. Res.*, vol. 47, no. 8, pp. 2446–2456, 2014.
[33] H. W. Lee, Y. Yoon, S. Park, et al., "Selective dispersion of high purity semiconducting single-walled carbon nanotubes with regioregular poly(3-alkylthiophene)s," *Nat. Commun.*, vol. 2, no. 1, p. 541, 2011.
[34] B. Mirka, D. Fong, N. A. Rice, O. A. Melville, A. Adronov, and B. H. Lessard, "Polyfluorene-sorted semiconducting single-walled carbon nanotubes for applications in thin-film transistors," *Chem. Mater.*, vol. 31, no. 8, pp. 2863–2872, 2019.
[35] W. Gomulya, G. D. Costanzo, E. J. F. de Carvalho, et al., "Semiconducting single-walled carbon nanotubes on demand by polymer wrapping," *Adv. Mater.*, vol. 25, no. 21, pp. 2948–2956, 2013.
[36] H. Ozawa, N. Ide, T. Fujigaya, Y. Niidome, and N. Nakashima, "One-pot separation of highly enriched (6, 5)-single-walled carbon nanotubes using a fluorene-based copolymer," *Chem. Lett.*, vol. 40, no. 3, pp. 239–241, 2011.
[37] T. Umeyama, N. Kadota, N. Tezuka, Y. Matano, and H. Imahori, "Photoinduced energy transfer in composites of poly [(*p*-phenylene-1, 2-vinylene)-co-(*p*-phenylene-1, 1-vinylidene)]

and single-walled carbon nanotubes," *Chem. Phys. Lett.*, vol. 444, nos. 4–6, pp. 263–267, 2007.
[38] Y. K. Kang, O.-S. Lee, P. Deria, et al., "Helical wrapping of single-walled carbon nanotubes by water soluble poly (*p*-phenyleneethynylene)," *Nano Lett.*, vol. 9, no. 4, pp. 1414–1418, 2009.
[39] P. He, S. Shimano, K. Salikolimi, et al., "Noncovalent modification of single-walled carbon nanotubes using thermally cleavable polythiophenes for solution-processed thermoelectric films," *ACS Appl. Mater. Interfaces*, vol. 11, no. 4, pp. 4211–4218, 2018.
[40] Y. H. Kwon, K. Minnici, J. J. Park, et al., "SWNT anchored with carboxylated polythiophene "Links" on high-capacity Li-ion battery anode materials," *J. Am. Chem. Soc.*, vol. 140, no. 17, pp. 5666–5669, 2018.
[41] H. Shi, L. Du, W. Xiong, M. Dai, W. K. Chan, and D. L. Phillips, "Study of electronic interactions and photo-induced electron transfer dynamics in a metalloconjugated polymer–single-walled carbon nanotube hybrid by ultrafast transient absorption spectroscopy," *J. Mater. Chem.*, vol. 5, no. 35, pp. 18527–18534, 2017.
[42] J. K. Sprafke, S. D. Stranks, J. H. Warner, R. J. Nicholas, and H. L. Anderson, "Noncovalent binding of carbon nanotubes by porphyrin oligomers," *Angew. Chem. Int. Ed.*, vol. 50, no. 10, pp. 2313–2316, 2011.
[43] H. Ozawa, X. Yi, T. Fujigaya, Y. Niidome, T. Asano, and N. Nakashima, "Supramolecular hybrid of gold nanoparticles and semiconducting single-walled carbon nanotubes wrapped by a porphyrin-fluorene copolymer," *J. Am. Chem. Soc.*, vol. 133, no. 37, pp. 14771–14777, 2011.
[44] J. H. Olivier, J. Park, P. Deria, et al., "Unambiguous diagnosis of photoinduced charge carrier signatures in a stoichiometrically controlled semiconducting polymer-wrapped carbon nanotube assembly," *Angew. Chem.*, vol. 127, no. 28, pp. 8251–8256, 2015.
[45] C.-K. Mai, B. Russ, S. L. Fronk, et al., "Varying the ionic functionalities of conjugated polyelectrolytes leads to both *p*- and *n*-type carbon nanotube composites for flexible thermoelectrics," *Energy Environ. Sci.*, vol. 8, no. 8, pp. 2341–2346, 2015.
[46] A. J. Ferguson, J. L. Blackburn, J. M. Holt, et al., "Photoinduced energy and charge transfer in P3HT:SWNT composites," *J. Phys. Chem. Lett.*, vol. 1, no. 15, pp. 2406–2411, 2010.
[47] M. Bernardi, M. Giulianini, and J. C. Grossman, "Self-assembly and its impact on interfacial charge transfer in carbon nanotube/P3HT solar cells," *ACS Nano*, vol. 4, no. 11, pp. 6599–6606, 2010.
[48] N. M. Dissanayake and Z. Zhong, "Unexpected hole transfer leads to high efficiency single-walled carbon nanotube hybrid photovoltaic," *Nano Lett.*, vol. 11, no. 1, pp. 286–290, 2011.
[49] H. Gu and T. M. Swager, "Fabrication of free-standing, conductive, and transparent carbon nanotube films," *Adv. Mater.*, vol. 20, no. 23, pp. 4433–4437, 2008.
[50] J. Geng and T. Zeng, "Influence of single-walled carbon nanotubes induced crystallinity enhancement and morphology change on polymer photovoltaic devices," *J. Am. Chem. Soc.*, vol. 128, no. 51, pp. 16827–16833, 2006.
[51] A. T. Mallajosyula, S. S. K. Iyer, and B. Mazhari, "Role of single walled carbon nanotubes in improving the efficiency of poly-(3-hexylthiophene) based organic solar cells," *J. Appl. Phys.*, vol. 108, no. 9, p. 094902, 2010.
[52] T. Schuettfort, H. Snaith, A. Nish, and R. Nicholas, "Synthesis and spectroscopic characterization of solution processable highly ordered polythiophene–carbon nanotube nanohybrid structures," *Nanotechnology*, vol. 21, no. 2, p. 025201, 2009.
[53] S. D. Stranks, C. Weisspfennig, P. Parkinson, M. B. Johnston, L. M. Herz, and R. J. Nicholas, "Ultrafast charge separation at a polymer–single-walled carbon nanotube molecular junction," *Nano Lett.*, vol. 11, no. 1, pp. 66–72, 2011.
[54] S. Kahmann, J. M. Salazar Rios, M. Zink, et al., "Excited-state interaction of semiconducting single-walled carbon nanotubes with their wrapping polymers," *J. Phys. Chem. Lett.*, vol. 8, no. 22, pp. 5666–5672, 2017.
[55] J. Bartelmess, C. Ehli, J.-J. Cid, et al., "Tuning and optimizing the intrinsic interactions between phthalocyanine-based PPV oligomers and single-wall carbon nanotubes toward *n*-type/*p*-type," *Chem. Sci.*, vol. 2, no. 4, pp. 652–660, 2011.
[56] J. Bartelmess, C. Ehli, J.-J. Cid, et al., "Screening interactions of zinc phthalocyanine–PPV oligomers with single wall carbon nanotubes—a comparative study," *J. Mater. Chem.*, vol. 21, no. 22, pp. 8014–8020, 2011.
[57] C. Ehli, C. Oelsner, D. M. Guldi, et al., "Manipulating single-wall carbon nanotubes by chemical doping and charge transfer with perylene dyes," *Nat. Chem.*, vol. 1, no. 3, pp. 243–249, 2009.
[58] C. Oelsner, C. Schmidt, F. Hauke, M. Prato, A. Hirsch, and D. M. Guldi, "Interfacing strong electron acceptors with single wall carbon nanotubes," *J. Am. Chem. Soc.*, vol. 133, no. 12, pp. 4580–4586, 2011.
[59] K. Dirian, S. Backes, C. Backes, et al., "Naphthalenebisimides as photofunctional surfactants for SWCNTs—towards water-soluble electron donor–acceptor hybrids," *Chem. Sci.*, vol. 6, no. 12, pp. 6886–6895, 2015.
[60] P. Deria, J.-H. Olivier, J. Park, and M. J. Therien, "Potentiometric, electronic, and transient absorptive spectroscopic properties of oxidized single-walled carbon nanotubes helically wrapped by ionic, semiconducting polymers in aqueous and organic media," *J. Am. Chem. Soc.*, vol. 136, no. 40, pp. 14193–14199, 2014.
[61] M. Zheng and B. A. Diner, "Solution redox chemistry of carbon nanotubes," *J. Am. Chem. Soc.*, vol. 126, no. 47, pp. 15490–15494, 2004.
[62] Y. Bai, G. Bullard, J.-H. Olivier, and M. J. Therien, "Quantitative evaluation of optical free carrier generation in semiconducting single-walled carbon nanotubes," *J. Am. Chem. Soc.*, vol. 140, no. 44, pp. 14619–14626, 2018.
[63] Y. Bai, J.-H. Olivier, G. Bullard, C. Liu, and M. J. Therien, "Dynamics of charged excitons in electronically and morphologically homogeneous single-walled carbon nanotubes," *Proc. Natl. Acad. Sci. U.S.A.*, vol. 115, no. 4, pp. 674–679, 2018.
[64] T. V. Eremin, P. A. Obraztsov, V. A. Velikanov, T. V. Shubina, and E. D. Obraztsova, "Many-particle excitations in non-covalently doped single-walled carbon nanotubes," *Sci. Rep.*, vol. 9, no. 1, p. 14985, 2019.
[65] W. J. Xiong, L. L. Du, K. C. Lo, et al., "Control of electron flow direction in photoexcited cycloplatinated complex containing conjugated polymer-single-walled carbon nanotube hybrids," *J. Phys. Chem. Lett.*, vol. 9, no. 14, pp. 3819–3824, 2018.
[66] A. M. Rao, P. C. Eklund, S. Bandow, A. Thess, and R. E. Smalley, "Evidence for charge transfer in doped carbon nanotube bundles from Raman scattering," *Nature*, vol. 388, no. 6639, pp. 257–259, 1997.

[67] T. Umeyama, J. Baek, Y. Sato, et al., "Molecular interactions on single-walled carbon nanotubes revealed by high-resolution transmission microscopy," *Nat. Commun.*, vol. 6, no. 1, pp. 1–9, 2015.

[68] J. Park, P. Deria, and M. J. Therien, "Dynamics and transient absorption spectral signatures of the single-wall carbon nanotube electronically excited triplet state," *J. Am. Chem. Soc.*, vol. 133, no. 43, pp. 17156–17159, 2011.

[69] J. Chmeliov, J. Narkeliunas, M. W. Graham, G. R. Fleming, and L. Valkunas, "Exciton–exciton annihilation and relaxation pathways in semiconducting carbon nanotubes," *Nanoscale*, vol. 8, no. 3, pp. 1618–1626, 2016.

[70] L. Lüer, S. Hoseinkhani, D. Polli, J. Crochet, T. Hertel, and G. Lanzani, "Size and mobility of excitons in (6, 5) carbon nanotubes," *Nat. Phys.*, vol. 5, no. 1, pp. 54–58, 2009.